

Optimal Design and Cascading Failure Evaluation of Remedial Action Schemes

Aditya Rangarajan and Line Roald

Dept. of Electrical and Computer Engineering, University of Wisconsin-Madison, Madison, Wisconsin, USA

{arangarajan4, roald}@wisc.edu

Abstract—Remedial action schemes (RAS) are often seen as an alternative to building new transmission infrastructure to relieve congestion in the system. Consequently, there has been a rapid growth in the number of RAS in electric power systems across the world. However, most RAS rely on fixed parameters and hence cannot adapt to the rapidly evolving nature of the electric grid. In this paper, an optimization framework (RAS-SCOPF) to automate the RAS design procedure is proposed. The proposed framework is a mixed integer quadratic program (MIQP) that chooses a set of optimal RAS actions and minimizes load shed when a contingency occurs. The cost of operation of the RAS-SCOPF is compared against those of standard OPF and SCOPF formulations. Moreover, the risk of cascading failure for the different formulations are evaluated using a DC power flow based cascading failure simulator (CFS). The proposed framework is applied to the RTS-96 24-bus network. The inclusion of RAS allows the system to be operated at a lower cost while preventing any contingency from evolving into cascading blackouts.

Index Terms—System Integrity Protection Scheme, Remedial Action Schemes, Cascading Failure Simulator, MIQP

I. INTRODUCTION

The introduction of competitive electricity markets along with increasing electricity demand and renewable generation have led to increased stress on the existing transmission infrastructure. As a result, the electric power system is forced to operate closer to its limits. Since post-contingency security constraints are often the source of congestion, there is an increasing reliance on post-contingency control avoid post-contingency overloads and maintain secure system operation [1]. Post-contingency manual corrective actions of the operator (e.g., generator redispatch, adjusting transformer tap settings, etc) can be too slow to arrest the propagation of disturbances. This has led to the global adoption of fast-acting system-wide protection systems, called Remedial Action Schemes(RAS), to maintain reliability [2].

According to the North American Electric Reliability Corporation (NERC), RAS are automatic protection systems that detect abnormal system conditions and take predetermined and fast control actions, including but not limited to, generator rejection, load shedding, and line switching [3]. RAS are also commonly referred to as system integrity protection schemes (SIPS) or special protection systems (SPS). RAS can use measurements from and take remedial actions at remote locations of the system, and thus differ from local protection systems. Since RAS can reduce violations of post-contingency constraints, they are often viewed as an inexpensive alternative to building new transmission infrastructure

[4]. However, increasing the number of RAS increases the operational complexity and poses several challenges as the power system continues to evolve rapidly. Existing procedures for designing RAS are often slow, requiring numerous offline simulations to ensure that the proposed action is sufficient and does not interact adversely with existing RAS and other protection devices [4], [5]. As a result, parameters of RAS, such as the conditions specified to trigger the RAS and the type of actions taken, typically do not change during real-time operations [6]. The slow design procedure, coupled with the use of fixed control parameters, may prevent RAS from adapting to rapidly evolving grid conditions.

Recent research has sought to address some of the issues and risks associated with corrective action identification. To improve the RAS design procedure, [7] proposes a sensitivity-based method to generate a set of triggering conditions and generator tripping actions to address post-contingency line overloads. However, the proposed method manually identifies suitable RAS actions, which limits the number of contingencies, operating conditions and control actions that can be studied. Further, recent research has shown the utility of considering the risk of corrective action failure (i.e. the risk of post-contingency corrective actions not being implemented correctly) in identifying an optimal system dispatch [8], [9], [10]. These methods considers corrective generator re-dispatch as the only corrective action, which simplifies modelling and solution of the optimization problem. However, generator re-dispatch is typically neither automatic nor quick enough to be considered as a RAS.

In this paper, we extend the above studies by proposing an optimization framework to design RAS and develop a cascading failure simulation to assess risk of RAS misoperation.

Our first contribution is an extension of the traditional security constrained optimal power flow (SCOPF) to design and optimize RAS settings at an operational time frame, which we refer to as RAS-SCOPF. The RAS-SCOPF is a mixed-integer optimization problem which models system operations in three stages, namely (i) pre-contingency operation, (ii) intermediate (post-contingency, pre-RAS) operations, and (iii) post-contingency, post-RAS operations. An innovative aspect of this model is that the second stage includes a set of logical constraints that describes whether or not the RAS is triggered, with RAS actions as decision variables.

Our second contribution is to develop an cascading failure simulation to assess the risk of the RAS not working as

arXiv:2302.05490v1 [eess.SY] 10 Feb 2023

intended due to, e.g., unexpected operating conditions. Our cascading failure simulator is based on the DCSIMSEP simulator [11], but was reimplemented in Julia [12] and extended to include a model of the relevant RAS schemes.

Our third contribution is to demonstrate our proposed method in a case study on the IEEE RTS-96 single area system. First, we show that the proposed RAS-SCOPF method reduce both operating cost and cascading risk compared to the traditional OPF and SCOPF formulations. Second, we assess the risk of RAS misoperation under loading conditions different from what it was designed for. The results highlight the benefits of reoptimizing the RAS settings in operations.

The rest of the paper is structured as follows. Section II describes the mathematical formulation of the proposed optimization problem, while Section III discusses the set-up of the cascading simulations. Section IV presents the results of the case study, and Section V concludes the paper.

II. OPTIMAL DESIGN OF REMEDIAL ACTION SCHEMES

RAS schemes are typically used to mitigate the impact of particular contingencies on system operations, thus allowing more effective use of existing transmission capacity in normal operations. While RAS may resolve different kinds of post-contingency problems and may involve different kinds of control actions, we focus on alleviating post-contingency line overloads using generation tripping. Our optimization aims to optimally choose the RAS actions, i.e. which generators are tripped once the RAS is triggered. We assume that the RAS is triggered when the considered line is overloaded, regardless of what caused the line flow to exceed the limit. As a result, the RAS action is shared among all considered contingencies.

A. Formulation of the RAS-SCOPF

We consider a power system where the sets \mathcal{G} , \mathcal{B} and \mathcal{L} represent the generators, buses and lines in the system, and $|\mathcal{G}|$ represents the number of elements in \mathcal{G} . The parameters P_g^{max} and P_g^{min} represent the maximum and minimum generation limits, while P_{fij}^{max} is the maximum transmission line capacity. We use **bold fonts** for decision variables, with the vectors \mathbf{P}_g^o , $\boldsymbol{\theta}^o$ and \mathbf{P}_f^o representing the pre-contingency generation, voltage angles and power flows, respectively. Similar decision variables with superscripts i and c are used to represent the power flows in the intermediate and the post-RAS stage, respectively. Generator and voltage variables related to individual generator or buses are denoted with subscript i or j , e.g. \mathbf{P}_{gi}^o , while lines have double subscripts ij representing either ends of the line, e.g. \mathbf{P}_{fij}^o .

1) *Objective function*: The objective function is given by

$$\min \sum_{i \in \mathcal{G}} f_i(\mathbf{P}_{gi}^o) + \sum_{k \in \mathcal{C}} \left(\sum_{i \in \mathcal{B}} \gamma(\mathbf{P}_{di}^{c,k} - P_{di}^o) + \sum_{i \in \mathcal{G}} \rho(1 - z_{gi}^j) \right) \quad (1)$$

The first term represents the generation cost of normal operation, with

$$f_i(\mathbf{P}_{gi}^o) = c_{2,i}(\mathbf{P}_{gi}^o)^2 + c_{1,i}\mathbf{P}_{gi}^o$$

where $c_{2,i}$ and $c_{1,i}$ are the quadratic and linear cost coefficients of generator i , respectively. The second term penalizes post-contingency load shedding, with P_{di}^o representing the normal load and $\mathbf{P}_{di}^{c,k}$ representing load served after a RAS is triggered. The parameter γ represents the load shedding cost. The third term minimizes the magnitude of the RAS action, represented as the number of generators tripped multiplied by a penalty factor ρ .

2) *Pre-contingency operating constraints*: We use a DC power flow model to model our system. The pre-contingency nodal power balance and power flows are given by

$$\mathbf{P}_{gi}^o - P_{di}^o = \sum_{j \in \mathcal{B}} \mathbf{P}_{fij}^o \quad \forall i \in \mathcal{B} \quad (2)$$

$$\mathbf{P}_{fij}^o = -b_{ij}(\boldsymbol{\theta}_i^o - \boldsymbol{\theta}_j^o) \quad \forall ij \in \mathcal{L} \quad (3)$$

where b_{ij} is the admittance of line ij . Generator and line limits are enforced by

$$P_{gi}^{min} \leq \mathbf{P}_{gi}^o \leq P_{gi}^{max} \quad \forall i \in \mathcal{G} \quad (4)$$

$$-P_{fij}^{max} \leq \mathbf{P}_{fij}^o \leq P_{fij}^{max} \quad \forall ij \in \mathcal{L} \quad (5)$$

3) *Intermediate operating constraints*: We next model the intermediate operating condition just after each contingency (prior to the implementation of any RAS). These constraints are included for all contingencies $k \in \mathcal{C}$, where \mathcal{C} is the set of all contingencies. The subset of critical contingencies that the RAS is designed to protect against is denoted by $\mathcal{C}_M \subset \mathcal{C}$.

To make up for generation imbalances following a generation or load outage, we assume a distributed slack model and redispatch generators using pre-determined participation factors K_i . The new generation levels $\mathbf{P}_g^{i,k}$ and associated generation limit constraints are given by

$$\mathbf{P}_{gi}^{i,k} = \mathbf{P}_{gi}^o + K_i \left[\sum_{i \in \mathcal{B}} (P_{di}^{i,k} - P_{di}^o) + \sum_{i \in \mathcal{G}} (\mathbf{P}_{gi}^o - \mathbf{P}_{gi}^{i,k}) + \Delta^i \right], \quad \forall i \in \mathcal{G}, k \in \mathcal{C} \quad (6)$$

$$P_{gi}^{min} \leq \mathbf{P}_{gi}^{i,k} \leq P_{gi}^{max}, \quad \forall i \in \mathcal{G}, k \in \mathcal{C} \quad (7)$$

where \mathcal{G}_k is the set of online generators after contingency k and the variable Δ^i represents the power mismatch in the network that arises because the participation factors K_i of the online generators may not sum to 1. The intermediate power balance and power flow constraints are given by

$$\mathbf{P}_{gi}^{i,k} - P_{di}^{i,k} = \sum_{j \in \mathcal{B}} \mathbf{P}_{fij}^{i,k} \quad \forall i \in \mathcal{B}, k \in \mathcal{C} \quad (8)$$

$$\mathbf{P}_{fij}^{i,k} = -b_{ij}(\boldsymbol{\theta}_{i,k}^i - \boldsymbol{\theta}_{j,k}^i) \quad \forall ij \in \mathcal{L}_k, k \in \mathcal{C} \quad (9)$$

where \mathcal{L}_k is the set of non-outaged lines in contingency k . For the contingencies the RAS is designed to protect against, denoted by \mathcal{C}_M , we do not enforce power flow limits, as we assume there may be overloads. For all other contingencies $k \in \mathcal{C} \setminus \mathcal{C}_M$, we enforce post-contingency line limits,

$$-P_{fij}^{max} \leq \mathbf{P}_{fij}^{i,k} \leq P_{fij}^{max} \quad \forall ij \in \mathcal{L}, k \in \mathcal{C} \setminus \mathcal{C}_M \quad (10)$$

4) *RAS design and triggering constraints*: In the intermediate stage, we also include constraints to evaluate whether the RAS is triggered by an overload. These constraints are included for all lines in the set of monitored lines, denoted by \mathcal{L}_M , and for the contingencies \mathcal{C}_M . Note that the set \mathcal{L}_M can include one or more lines. The following logic constraints assess whether the loading on a monitored line $ij \in \mathcal{L}_M$ exceeds its maximum loading after a contingency k ,

$$P_{fij}^{i,k} - P_{fij}^{max} \geq m(1 - z_{1,ij}^k) \quad \forall ij \in \mathcal{L}_M, k \in \mathcal{C}_M \quad (11)$$

$$P_{fij}^{i,k} - P_{fij}^{max} \leq Mz_{1,ij}^k \quad \forall ij \in \mathcal{L}_M, k \in \mathcal{C}_M \quad (12)$$

$$-P_{fij}^{i,k} - P_{fij}^{max} \geq m(1 - z_{2,ij}^k) \quad \forall ij \in \mathcal{L}_M, k \in \mathcal{C}_M \quad (13)$$

$$-P_{fij}^{i,k} - P_{fij}^{max} \leq Mz_{2,ij}^k \quad \forall ij \in \mathcal{L}_M, k \in \mathcal{C}_M \quad (14)$$

$$z_{1,ij}^k + z_{2,ij}^k \geq z_{3,ij}^k \quad \forall ij \in \mathcal{L}_M, k \in \mathcal{C}_M \quad (15)$$

$$z_{1,ij}^k + z_{2,ij}^k \leq z_{3,ij}^k \quad \forall ij \in \mathcal{L}_M, k \in \mathcal{C}_M \quad (16)$$

Eqs. (11) and (12) set the variable $z_{1,ij}^k = 1$ if the line is overloaded in the positive flow direction, and $z_{1,ij}^k = 0$ otherwise. Eqs. (13), (14) and $z_{2,ij}^k \in \{0, 1\}$ enforce the same condition for the negative flow direction. If the line is overloaded in either direction, (15) and (16) set $z_{3,ij}^k = 1$ to indicate that contingency k causes a RAS-triggering condition on line ij , and ensure that $z_{3,ij}^k = 0$ otherwise. The parameters M and m are big-M constants that represent valid lower and upper bounds on the left hand side of the constraints.

The binary variable y_j^k indicates whether the j^{th} RAS scheme has been triggered. Specifically, $y_j^k = 1$ if $z_{3,ij}^k = 1$ for one or more lines in the monitored set \mathcal{L}_M^j and $y_j^k = 0$ otherwise. For all $k \in \mathcal{C}_M$, this condition is expressed by

$$\sum_{(i,j) \in \mathcal{L}_M^j} z_{3,ij}^k \geq y_j^k \quad \sum_{(i,j) \in \mathcal{L}_M^j} z_{3,ij}^k \leq |\mathcal{L}_M^j| y_j^k \quad (17)$$

For the j^{th} RAS scheme, we assume that at least one generator should be tripped, i.e.,

$$\sum_{i \in \mathcal{G}} z_{gi}^j \leq |\mathcal{G}| - 1 \quad (18)$$

where z_{gi}^j represents the post-RAS status of generator $i \in \mathcal{G}$. If the generator is still operating, $z_{gi}^j = 1$ and otherwise $z_{gi}^j = 0$.

5) *Post-RAS constraints*: For all contingencies $k \in \mathcal{C}_M$, if $y_j^k = 1$ and the j^{th} RAS is triggered after contingency k , we enforce that the generators are tripped as described by (18),

$$z_{gi}^k - z_{gi}^j \leq (1 - y_j^k) \quad z_{gi}^k - z_{gi}^j \geq (y_j^k - 1) \quad (19)$$

If the RAS is not tripped, i.e. $y_j^k = 0$, all generators will remain in operation,

$$\sum_{i \in \mathcal{G}} z_{gi}^k \geq |\mathcal{G}|(1 - y_j^k) \quad (20)$$

In addition to generator tripping, we also allow load shedding as an emergency action, i.e.,

$$P_{di}^{i,k}(1 - y_j^k) \leq P_{di}^{c,k} \leq P_{di}^{i,k} \quad \forall i \in \mathcal{B} \quad (21)$$

The load shedding may differ between contingencies, but is penalized with a very high value γ in the objective function.

To manage the imbalance following the generation trip triggered by the RAS as well as load shedding, we again use adjustments based on droop factors K_i , i.e.

$$P_{gi}^{c,k} = P_{gi}^{i,k} + K_i \left[\sum_{i \in \mathcal{B}} (P_{di}^{c,k} - P_{di}^{i,k}) + \sum_{i \in \mathcal{G}} (P_{gi}^{i,k} - P_{gi}^{c,k}) + \Delta^c \right] \quad (22)$$

We enforce that the generation levels either respect the generation limits or are set to zero if the generator is tripped,

$$z_{gi}^k P_{gi}^{min} \leq P_{gi}^{c,k} \leq z_{gi}^k P_{gi}^{max} \quad (23)$$

The power flow in the post-RAS conditions is represented by

$$P_{gi}^{c,k} - P_{di}^{c,k} = \sum_{j \in \mathcal{B}} P_{fij}^{c,k} \quad (24)$$

$$P_{fij}^{c,k} = -b_{ij}(\theta_{i,k}^c - \theta_{j,k}^c) \quad (25)$$

$$-P_{fij}^{max} \leq P_{fij}^{c,k} \leq P_{fij}^{max} \quad (26)$$

To summarize, the RAS-SCOPF minimizes the pre-contingency operation cost and chooses the smallest RAS action that reduces load shedding and maintains secure operation against a set of specified contingencies. Since the pre-contingency operation cost is a quadratic function of the pre-contingency generation, the resulting problem is a mixed integer quadratic program (MIQP).

B. Benchmark formulations

To assess the performance of the RAS-SCOPF, we compare its performance against a traditional DC OPF and a DC SCOPF, as described below.

1) *OPF*: The OPF minimizes pre-contingency generation cost,

$$\min \sum_{i \in \mathcal{G}} f_i(P_{gi}^o) \quad (27)$$

subject only to the pre-contingency constraints (2)-(5).

2) *SCOPF*: The SCOPF minimizes the pre-contingency generation cost (27) subject to the pre-contingency constraints (2)-(5) and security constraints (6)-(10). to ensure that the system will operate without violations immediately after any contingency has occurred, and we set $\mathcal{C}_M = 0$.

3) *RAS-aware SCOPF*: The RAS-aware SCOPF is a modified version of the SCOPF that does not include the normal security constraints for contingencies $k \in \mathcal{C}_M$. The RAS-aware SCOPF minimizes pre-contingency generation cost (27) subject to the pre-contingency constraints (2)-(5) and security constraints (6)-(10) for $k \in \mathcal{C} \setminus \mathcal{C}_M$. For contingencies $k \in \mathcal{C}_M$, the RAS-aware SCOPF ensures feasibility of post-RAS generation redispatch by enforcing

$$P_{gi}^o + r_i \leq P_{gi}^{max} \quad \forall i \in \mathcal{G}, k \in \mathcal{C}_M \quad (28)$$

$$r_i \geq K_i \Delta P_g \quad \forall i \in \mathcal{G}, k \in \mathcal{C}_M \quad (29)$$

$$\Delta P_g = \sum_{i \in \mathcal{G}_{RAS}} P_{gi}^o \quad \forall k \in \mathcal{C}_M \quad (30)$$

where r_i is a reserve capacity needed to handle RAS activation and \mathcal{G}_{RAS} is the set of generators tripped by the RAS.

III. CASCADING SIMULATION

Modelling cascading failures in power systems is challenging because there are several ways in which an initiating contingency can evolve into a series of cascading outages, e.g., cascading thermal overloads, voltage instability, transient instability, hidden failures in protection systems or human errors [13], [14]. Here, we focus on cascading events driven by thermal overloads, as our goal is to evaluate the effectiveness of a RAS scheme in preventing such cascading events. We base our cascading simulator on a DC power flow model, which is computationally very efficient and hence widely used to assess system behaviour when subjected to multiple contingencies and operating conditions. The drawback of using a DC power flow based model is that it does not capture reactive power and voltage variability, and also assumes that the system reaches a steady-state after every contingency. Thus, DC models cannot capture the effects of dynamic phenomena like voltage and transient instability, or in situations where a steady-state solution does not exist. However, in the early stages of a cascade, before the loss of dynamic stability, the DC power flow models can describe the evolution of the system with good accuracy. Thus, choosing an appropriate definition of system failure helps limit the difference between actual system behaviour and that predicted by models based on DC power flow approximations in the case of cascading overloads [15].

Figure 1 illustrates the cascading failure simulator designed to test the performance of the designed RAS. Our simulator builds on DCSIMSEP [11]. A major difference between DCSIMSEP and our simulator is RAS modelling, which is absent in DCSIMSEP. Another difference includes the way in which generators and loads are redispatched, which we do by solving the optimization problem (31)-(39). Further, our simulator does not model overcurrent relays to track the time elapsed between successive outages.

The steps involved in a cascading simulation are summarized in Fig. 1 and described below in more detail:

Step 0: Initialization At the beginning of the simulation, the system has to be initialized appropriately. When evaluating the risk of cascading failures of the different formulations, the system is initialized using the RAS-SCOPF, OPF or SCOPF, respectively. When analysing the effectiveness of the RAS for different loading conditions, the system is initialized with the solutions of the RAS-aware SCOPF.

Step 1: Apply a contingency We apply an $n - 1$ contingency to the system by modifying the status of the outaged line.

Step 2: Check for system failure We calculate the line admittance matrix B^F considering all outages in the system and identify all the resulting islands. Here, we define system failure as the state when at least 10% of the buses are disconnected from the largest island. If the system satisfies the chosen definition of system failure, terminate the simulation. If it is not satisfied, continue to step 3.

Step 3: Implement RAS action If the applied contingency causes overloads in any one of the lines monitored by a RAS, this RAS is triggered. In this case, we trip generators according

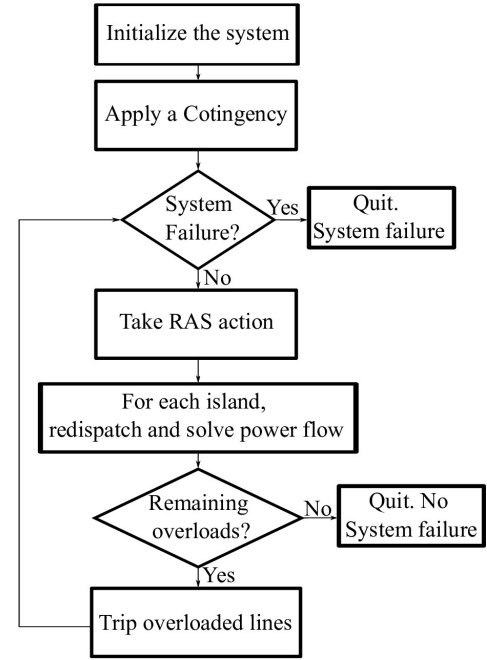


Fig. 1. Flowchart for the Cascading Failure Simulator

to the pre-defined RAS action and shed the necessary amount of load. If there are no RAS present in the system or if the RAS has already been triggered, we do nothing.

Step 4: Redispatch generators and load If there is a mismatch between load and generation because the system is separated into several islands or a RAS scheme has lead to generation tripping and load shed, we redispatch generators and loads in every island by solving the following optimization problem:

$$\min \sum_{i \in \mathcal{B}_{isl}} P_{di}^n - P_{di}^o + \sum_{i \in \mathcal{G}_{isl}} (1 - z_{gi}^n) \quad (31)$$

subject to

$$\text{for all generators in the island } i \in \mathcal{G}_{isl} \quad (32)$$

$$z_{gi}^n \leq z_{gi}^o \quad (33)$$

$$P_{gi}^n - \left(P_{gi}^o + K_i \sum_{i \in \mathcal{B}_{isl}} (P_{di}^n - P_{di}^o) + K_i \left[\sum_{i \in \mathcal{G}_{isl}} (P_{gi}^n - P_{gi}^o) + \Delta \right] \right) \leq M(1 - z_{gi}^n) \quad (34)$$

$$P_{gi}^n - \left(P_{gi}^o + K_i \sum_{i \in \mathcal{B}_{isl}} (P_{di}^n - P_{di}^o) + K_i \left[\sum_{i \in \mathcal{G}_{isl}} (P_{gi}^n - P_{gi}^o) + \Delta \right] \right) \geq M(1 - z_{gi}^n) \quad (35)$$

$$\sum_{i \in \mathcal{G}_{isl}} P_{gi}^n = \sum_{i \in \mathcal{B}_{isl}} P_{di}^n \quad (36)$$

$$z_{gi}^n P_{gi}^{min} \leq P_{gi}^n \leq z_{gi}^n P_{gi}^{max} \quad (37)$$

$$\text{for all buses in the island } i \in \mathcal{B}_{isl} \quad (38)$$

$$0 \leq P_{di}^n \leq P_{di}^o \quad (39)$$

TABLE I
CRITICAL CONTINGENCIES AND POST-CONTINGENCY LOADING LEVEL ON OVERLOADED LINES

Outaged Line	23	7	18	21	22	27	29	25	26
Overloaded Line	7	23	23	23	23	23	23	28	28
Loading Level (% of Max)	102.02%	120.37%	100.84%	108.33%	111.00%	120.37%	108.18%	103.99%	103.99%

Here, the superscripts o and n refer to the generation and load before and after the redispatch respectively. Similar to the RAS-SCOPF, the generators are redispatched using a distributed slack bus model and participation factors K_i .

Step 5: Trip overloaded lines We solve a DC power flow to compute the line flows and identify all lines in the island that are overloaded. Because protective equipment for each line is assumed to have inverse time characteristics (i.e. it trips faster larger the overload), we trip only the line with the maximum overload, unless it is monitored by RAS and the RAS has not been triggered yet. Move to step 2).

IV. CASE STUDY

The RAS-SCOPF is used to design a remedial action scheme for the 24-bus system shown in Fig. 2. The system is based on the single area IEEE RTS-96 system described in [16], with some modifications. To make the case study more interesting, we reduce the line rating of all lines to 80% of the original capacities listed in [16]. This makes the system more congested, with a subset of contingencies causing post-contingency line overloads. We only consider line outage constraints on non-radial lines and the capacity of the radial line 11 (from bus 7 to 8) is increased to 150% of its original rating to ensure that it is never binding. While designing the RAS, we consider only the peak load scenario with a total load of 2850 MW. We assume that only generators 1-16 are responsible for maintaining power balance in the system. For these generators, we define non-zero participation factors based on their maximum generation capacity,

$$K_i = \frac{P_{gi}^{max}}{\sum_{k=1}^{16} P_{gk}^{max}} \quad \text{for } i = 1, \dots, 16. \quad (40)$$

We assume a fixed penalty $\gamma = \$5000/\text{MW}$ for load shedding and a fixed cost $\rho = \$1000$ for every generator that is shed from the network. We set $M = -m = 100$ p.u..

A. RAS design

Table I shows all the contingencies that would result in post-contingency overloads on other lines, assuming the initial dispatch is obtained using the OPF formulation. We observe that there are several different contingencies that lead to an overload on line 23. We therefore demonstrate our proposed method by designing a RAS scheme that monitors overloads on this line. The set of contingencies \mathcal{C}_M which the RAS is designed to protect against thus corresponds to the outages of lines $\{7, 18, 21, 22, 27, 29\}$. Fig. 2 shows the location of the monitored line (in green) and the lines that correspond to the critical contingencies (in red).

Solving the RAS-SCOPF with a single RAS scheme on line 23 and the given set of contingencies, we obtain a solution with

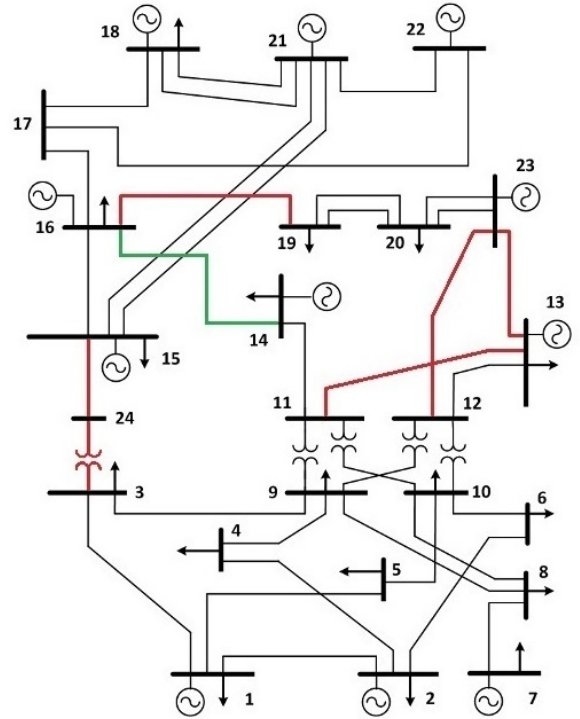


Fig. 2. IEEE RTS-96 24-bus system. Line 23 is shown in green and the lines whose outages cause overloads in line 23 are shown in red

pre-contingency generation cost \$62784.0. When detecting an overload in line 23, the RAS trips the generator $\mathcal{G}_{RAS} = \{22\}$, which corresponds to a 155 MW of generation capacity. The resulting power imbalance is balanced by generators 1-16, and does not cause any further overloads or load shed. As a result, we declare that our RAS scheme is effective.

B. Comparison with other OPF formulations

We next compare the RAS-SCOPF to the OPF and SCOPF formulations described in Section II.B. We first solve each optimization problem and observe the corresponding pre-contingency generation costs and then evaluate the risk of post-contingency cascading failure by running cascading simulations for all contingencies listed in Table I.

Table II shows the pre-contingency generation cost for the three OPF formulations. Dispatching generators using the OPF results in the lowest pre-contingency operating cost of the system. The RAS-SCOPF results in 3% higher pre-contingency costs than the OPF, as it needs to ensure that the generator redispatch after the RAS action is feasible and that the initial dispatch is secure against critical contingencies that do not trigger the RAS. However, the cost of the RAS-

TABLE II
COMPARISON OF DIFFERENT OPF FORMULATIONS

Formulation	OPF	RAS-SCOPF	SCOPF
Operational Cost	\$61001.2	\$62784.0	\$68197.4
Cost increase relative to OPF (%)	0%	2.92%	11.8%
Number of contingencies leading to load shed	9	0	0
Total load shed	7832.8	0	0

SCOPF is significantly lower than the SCOPF, which results in a cost increase of nearly 12%. This is because the SCOPF needs to ensure that all contingency constraints are satisfied without post-contingency generation tripping actions. When considering the outcome of the cascading simulations for each solution, also listed in Table II, we observe that the low-cost OPF solution has a significantly higher risk of cascading failure than the other two solutions. When the generators are dispatched using OPF, all the contingencies listed in Table I result in cascading failure with a total load shed of 7832.8 MW across all contingencies. With the RAS-SCOPF and the SCOPF, none of the contingencies result in a cascading failure. Based on these results, we conclude that the RAS we designed reduces operational costs relative to the SCOPF solution and lowers the risk of cascading failure relative to the OPF solution.

C. Sensitivity to load distribution

When designing the RAS, we only consider the peak load scenario. To assess how the RAS performs under different load conditions, cascade simulations are run for a range of loading conditions. To vary the load distribution, we first scale the load at every bus by a factor that is randomly drawn from a uniform distribution X , and then rescale the load to ensure that the total load in the system remains at 2850 MW,

$$P_{di}^n = X_i P_{di}^o \frac{\sum_{\ell \in \mathcal{B}} P_{d\ell}^o}{\sum_{j \in \mathcal{B}} P_{dj}^n} \quad \text{for } i \in \mathcal{B}. \quad (41)$$

When studying the performance of RAS when subjected to small load disturbances, $X \sim U(0.9, 1.1)$, while $X \sim U(0.5, 1.5)$ for larger load disturbances. For each load scenario, the system is initialized by solving the RAS-aware SCOPF. Any scenario that renders the RAS-aware SCOPF infeasible is discarded.

When load deviations are small ($X \sim U(0.9, 1.1)$), around 70% (68 out of 100) of scenarios have a feasible solution to the RAS-aware SCOPF. For most of the feasible load scenarios, the RAS is capable of preventing any critical contingency listed in table I from evolving into a cascading event. However, there are 3 load scenarios where, for at least one critical contingency, the RAS action is not sufficient to remove the overload on line 23 resulting in a cascading failure. The total load shed across these scenarios is 1399.2 MW.

In the case of larger load deviation ($X \sim U(0.5, 1.5)$), only 55% (55 out of 100) of the scenarios have a feasible solution

to the RAS-aware SCOPF. Among those scenarios, there are many that lead to cascading events after an initial line outage. Since outage of line 7 causes the largest overload in line 23, results pertaining only to the outage of line 7 are presented. The results are similar for all other contingencies in the set \mathcal{C}_M , except that fewer scenarios result in cascading failure.

Out of the 55 feasible scenarios, there are 16 scenarios where the RAS action is not sufficient to prevent cascading failure when line 7 is outaged. In all these cases, RAS was not able to remove the overload in line 23, resulting in overloads on other lines and eventually lead to cascading failure. For example, in one of the scenarios, the outage of line 7 triggers the RAS but the RAS action is insufficient to alleviate the overload on line 23. Thus, line 23 is tripped, followed by subsequent outages of lines 22 and 21 resulting in a total load shed of 1013.6 MW. The scenario described above was the worst case observed across all scenarios and contingencies.

In 11 additional load scenarios, the outage of line 7 causes overloads in lines that are not monitored by the RAS. These overloads do not trigger the RAS, but cause cascading outages involving other lines. In these cases, the system has separated into multiple islands and a significant amount load shed (up to 14.5%) occurs.

From these results, we could conclude that the RAS schemes either should be designed to be robust to large deviations in the loading condition, or that the RAS actions should be updated to reflect changing loading conditions using, e.g., the RAS-SCOPF.

V. CONCLUSIONS

Remedial action schemes (RAS) are an important tool to reduce congestion in power systems operation. However, RAS pose several challenges to grid operators due to their inability to adapt to changing conditions and the added risk of implementation failure. To address these challenges, we propose the RAS-SCOPF to choose a set of optimal RAS actions in response to current loading conditions. We further implement a DC power flow based cascading failure simulator to evaluate the risk of cascading failure when the RAS is present in the system and when it is not.

The proposed method is applied to the RTS-96 24-bus network. Using the RAS-SCOPF lowered operational costs compared to the SCOPF, while ensuring same level of security against all critical contingencies. We further observe that the RAS designed using RAS-SCOPF is robust against small deviations in load, with very few scenarios resulting in system failure. However, the RAS was designed for only a single load scenario and is not effective in preventing cascading failures for loading scenarios that differ too much from the design scenario. This demonstrates the need for considering several load scenarios when solving the RAS-SCOPF or updating the RAS actions in real time.

In future work, we aim to develop algorithms that solve the RAS-SCOPF efficiently for larger systems and multiple scenarios, while accounting for the RAS failure probabilities.

REFERENCES

- [1] P. Panciatici, M. Campi, S. Garatti, S. Low, D. Molzahn, A. Sun, and L. Wehenkel, "Advanced optimization methods for power systems," in *2014 Power Systems Computation Conference*, 2014, pp. 1–18.
- [2] V. Madani, D. Novosel, S. Horowitz, M. Adamiak, J. Amantegui, D. Karlsson, S. Imai, and A. Apostolov, "Ieee prsr report on global industry experiences with system integrity protection schemes (sips)," *IEEE Trans on Power Delivery*, vol. 25, no. 4, pp. 2143–2155, 2010.
- [3] NERC, "Glossary of terms used in nerc reliability standards," 2022. [Online]. Available: https://www.nerc.com/pa/Stand/Glossary_of_Terms/Glossary_of_Terms.pdf
- [4] J. McCalley, O. Oluwaseyi, V. Krishnan, R. Dai, C. Singh, and K. Jiang, "System protection schemes: limitations, risks, and management," *Final Report to the Power Systems Engineering Research Center (PSERC)*, 2010.
- [5] J. McCalley and W. Fu, "Reliability of special protection systems," *IEEE Trans on Power Systems*, vol. 14, no. 4, pp. 1400–1406, 1999.
- [6] J. O'Brien, R. Huang, E. Barrett, Q. Huang, X. Fan, and R. Diao, "Survey on ras/sps modeling practice," 2017.
- [7] H. Li, K. Shetye, T. Overbye, K. Davis, and S. Hossain-Mckenzie, "Towards the automation of remedial action schemes design," 2021.
- [8] E. Karangelos, P. Panciatici, and L. Wehenkel, "Whither probabilistic security management for real-time operation of power systems?" in *2013 IREP Symposium Bulk Power System Dynamics and Control - IX Optimization, Security and Control of the Emerging Power Grid*, 2013, pp. 1–17.
- [9] E. Karangelos and L. Wehenkel, "Probabilistic reliability management approach and criteria for power system real-time operation," in *2016 Power Systems Computation Conference (PSCC)*, 2016, pp. 1–9.
- [10] —, "An iterative ac-scopf approach managing the contingency and corrective control failure uncertainties with a probabilistic guarantee," *IEEE Trans on Power Systems*, vol. 34, no. 5, pp. 3780–3790, 2019.
- [11] M. J. Eppstein and P. D. H. Hines, "A "random chemistry" algorithm for identifying collections of multiple contingencies that initiate cascading failure," *IEEE Trans on Power Systems*, vol. 27, no. 3, pp. 1698–1705, 2012.
- [12] J. Bezanson, A. Edelman, S. Karpinski, and V. B. Shah, "Julia: A fresh approach to numerical computing," *SIAM review*, vol. 59, no. 1, pp. 65–98, 2017.
- [13] Vaiman, Bell, Chen, Chowdhury, Dobson, Hines, Papic, Miller, and Zhang, "Risk assessment of cascading outages: Methodologies and challenges," *IEEE Trans on Power Systems*, vol. 27, no. 2, pp. 631–641, 2012.
- [14] H. Haes Alhelou, M. E. Hamedani-Golshan, T. C. Njenda, and P. Siano, "A survey on power system blackout and cascading events: Research motivations and challenges," *Energies*, vol. 12, no. 4, 2019. [Online]. Available: <https://www.mdpi.com/1996-1073/12/4/682>
- [15] J. Yan, Y. Tang, H. He, and Y. Sun, "Cascading failure analysis with dc power flow model and transient stability analysis," *IEEE Trans on Power Systems*, vol. 30, no. 1, pp. 285–297, 2015.
- [16] C. Grigg, P. Wong, P. Albrecht, R. Allan, M. Bhavaraju, R. Billinton, Q. Chen, C. Fong, S. Haddad, S. Kuruganty, W. Li, R. Mukerji, D. Patton, N. Rau, D. Reppen, A. Schneider, M. Shahidepour, and C. Singh, "The ieee reliability test system-1996. a report prepared by the reliability test system task force of the application of probability methods subcommittee," pp. 1010–1020, 1999.